Global Optimization of Cerebral Cortex Layout

Supplementary Online Material

Christopher Cherniak*, Zekeria Mokhtarzada,
Raul Rodriguez-Esteban, B. K. Changizi

Functional areas of mammalian cerebral cortex seem positioned to minimize finely costs of their interconnections, down to a best-in-a-billion optimality level. Macaque and cat cortex rank better in connection optimization than the wiring of comparably structured computer chips, but somewhat worse than the economic commodity-flow network among U.S. states. Cortex wiring conforms to a Size Law better than the macroeconomic patterns, which may indicate cortex optimizing mechanisms involve more global processes.

Cortex Datasets

Macaque Visual Cortex

Cat Visual, Auditory, & Somatosensory Cortex

Cat Cortex Meta-Modules

Non-neural Datasets

AMI49 Microchip

Macroeconomic Commodity-Flow Network

Conclusion

References and Notes

* To whom correspondence should be addressed:

Committee for Philosophy and the Sciences, Department of Philosophy, University of Maryland, College Park, MD 20742, USA. cc27[at]wam[dot]umd[dot]edu

Next

Last Modified 11/19/2002

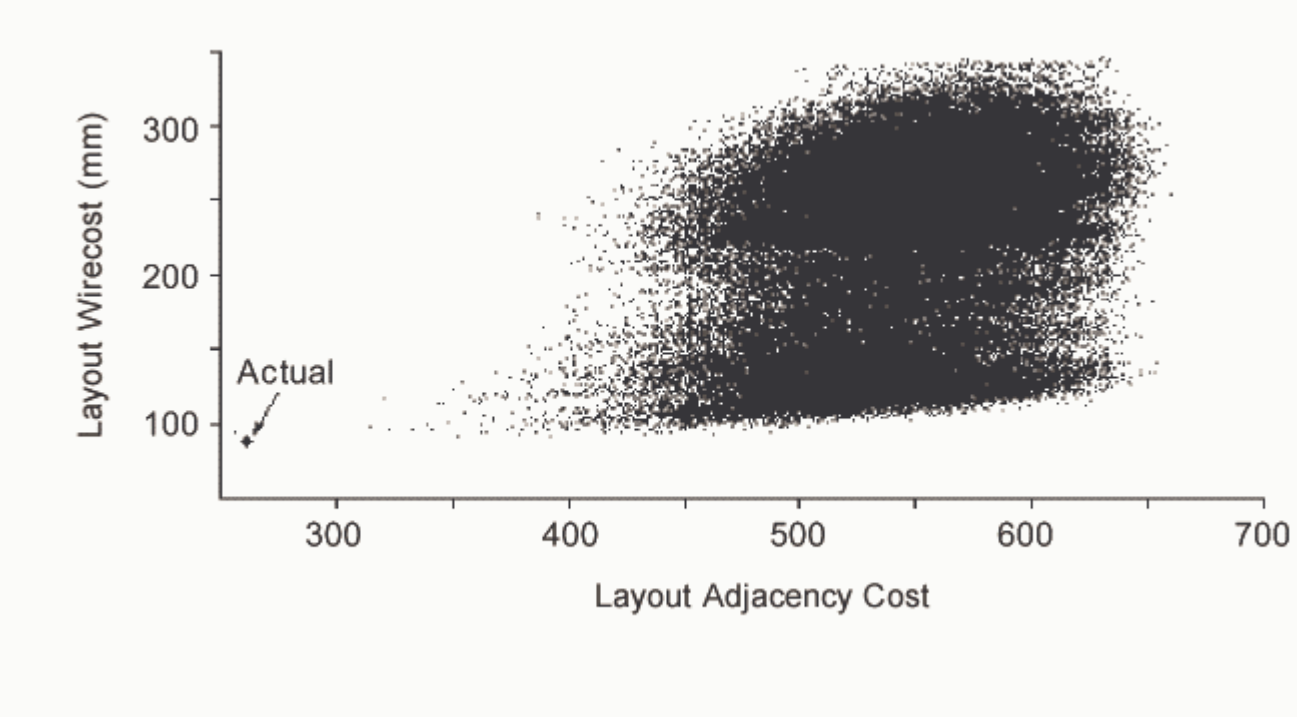

Enlarge

Fig. S1 . Adjacency rule conformance, vs total wirecost, of 100,000 C. elegans ganglion layouts randomly sampled from the set of all 11! possible layouts.(1) Adjacency rule: If two components are connected, then they are adjacent to each other.(1) A layout is scored in terms of its number of violations of this "all or nothing" adjacency rule. Correlation between good adjacency rule performance and cheap wirecost is not strong ($r^2 = 0.05$); generally, the adjacency rule is not an effective means to good wirecost. However, the small set of nematode nervous system layouts best fitting the adjacency rule--the points at the far left--behave markedly differently: they correspond closely to the best wirecost layouts. (The larger point at the far left of the dispersion diagram represents the actual, minimum-wirecost layout.) Thus, good adjacency rule scores are worth exploring as a surrogate for wirecost of layouts.

Previous | Next

Last Modified 11/19/2002

Fig. S2 . Parcellation of cerebral cortex of macaque. Connection-cost optimization analysis of layout of 17 core areas of the visual cortex (white), along with 10 immediately contiguous "edge" areas (dark gray): Placement of the interconnected functional areas is evaluated for how well total interconnection costs are minimized. 120 connections are reported among the core areas and with the edge areas. Core and edge areas are listed in Table S1 connection matrix below. Rostral is to right.(2)

Table S1 . Combined connection and adjacency matrix for macaque visual cortex. The series of 17 core visual areas shown above in Fig. S2 is listed (V1 - CITv), in the order in which the areas successively added to the analysis. They are followed by the set of 10 edge areas for the total core (PO - TH). Connections of an area to itself are excluded. A cell with 0 indicates no known connection between the area of that row and of that column; 1 indicates connection in one direction between the two areas; 2 indicates two-way connection. Cell values in **bold** designate topological contiguity of the two areas on the cortex sheet, as in Fig. S2.(3)

	V1	V2	V3	VP	V3a	V4	DP	VOT	V4t	MT	MSTd	MSTl	FST	PITd	PITv	CITd	CITv
V2	**2**																
V3	2	**2**															
VP	0	**2**	1														
V3a	2	2	**2**	2													
V4	2	**2**	**2**	**2**	**2**												
DP	0	0	0	0	**2**	**2**											
VOT	0	2	0	2	0	**1**	0										
V4t	1	1	2	0	0	**2**	0	0									
MT	2	2	2	2	2	2	0	0	**2**								
MSTd	0	2	2	2	2	0	2	0	1	**2**							
MSTl	0	2	0	0	2	0	1	0	1	**2**	**0**						
FST	0	1	2	1	2	2	1	0	2	**2**	2	**2**					
PITd	0	0	0	0	0	**2**	0	**1**	**0**	**0**	1	0	**1**				
PITv	0	0	0	0	0	2	0	**1**	0	0	1	0	1	**0**			
CITd	0	0	0	0	0	2	0	0	0	0	0	0	**0**	**0**	1		
CITv	0	0	0	0	0	2	0	0	0	0	0	0	0	1	**2**	**0**	
PO	2	**1**	**1**	1	1	0	2	0	1	1	2	2	0	0	0	0	0
PIP	2	**1**	**2**	2	**0**	2	2	0	0	2	0	0	0	0	0	0	0
LIP	0	0	2	1	1	2	**2**	0	0	2	2	1	2	0	1	0	0
7a	0	0	0	0	0	**0**	**2**	0	0	**0**	**2**	0	1	0	0	0	0
STPp	0	0	0	0	0	0	0	0	0	0	**2**	**2**	**2**	0	0	1	1
STPa	0	0	0	0	0	0	0	0	0	0	0	0	**0**	0	0	0	0
AITd	0	0	0	0	0	0	0	0	0	0	0	0	**0**	1	1	**1**	2
AITv	0	0	0	0	0	2	0	0	0	0	0	0	0	1	2	1	**2**
TF	0	**0**	2	**2**	0	**2**	0	**0**	0	0	1	0	2	0	**1**	0	**1**
TH	0	**0**	0	0	0	2	0	0	0	0	0	0	0	0	1	1	1

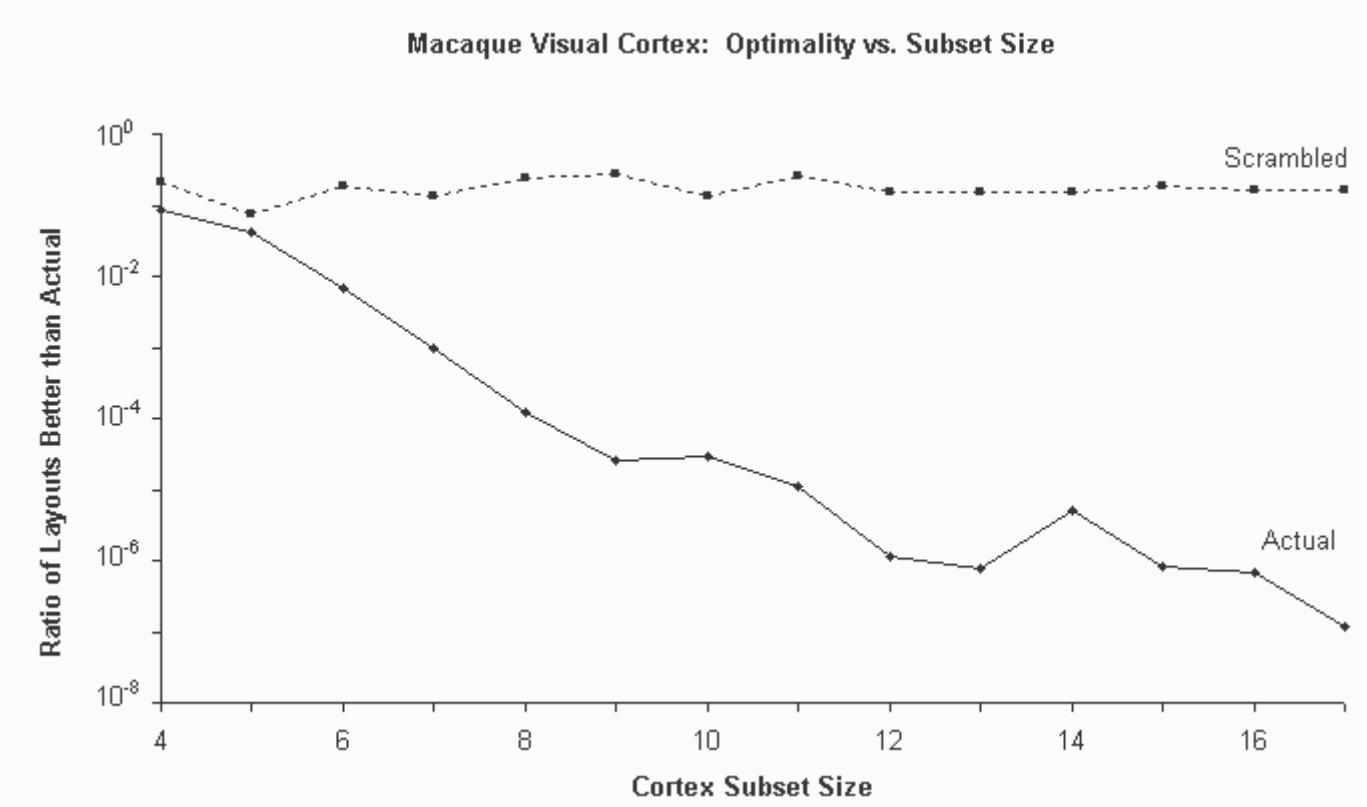

Fig. S3. Size Law for macaque visual cortex areas. The Size Law: If a set of connected components is optimally placed, then, the smaller a subset of that total layout, the less optimized it will tend to be. The system of components here is 17 contiguous macaque visual cortical areas as in Fig. S2, with connections and adjacencies as in Table S1. Optimality-measure is conformance of the system to the adjacency rule: If two components are connected, then they are adjacent to each other.(1) A layout is scored in terms of its number of violations of this "all or nothing" adjacency rule. A series of nested compact subsets of the set of cortical areas was generated, each consisting of from 4 to the full 17 areas. (Order of successive elements added is as in Table S1.) Each subset of the actual layout was compared with all possible alternative layouts of that subset for adjacency-rule optimality (16 and 17-element sets were each compared only with random samples of 10^9 alternative layouts).

The "Actual layout" curve shows that smaller subsets rank approximately in the middle of their group of alternative layouts. But, as subset size increases, optimality-ranking of the actual layout consistently improves (with two exceptions, $p < 0.02$). Fewer than one in a million of all alternative layouts conform to the adjacency rule better than the actual layout of the complete 17-component set. For comparison, the "Scrambled layout" broken-line curve shows the corresponding analysis for a layout of the 17 visual areas with their adjacencies randomly shuffled; no Size Law trend toward improving optimality is now evident. Note that this analysis includes only 17 of the total 73 cortical areas.

Previous | Next

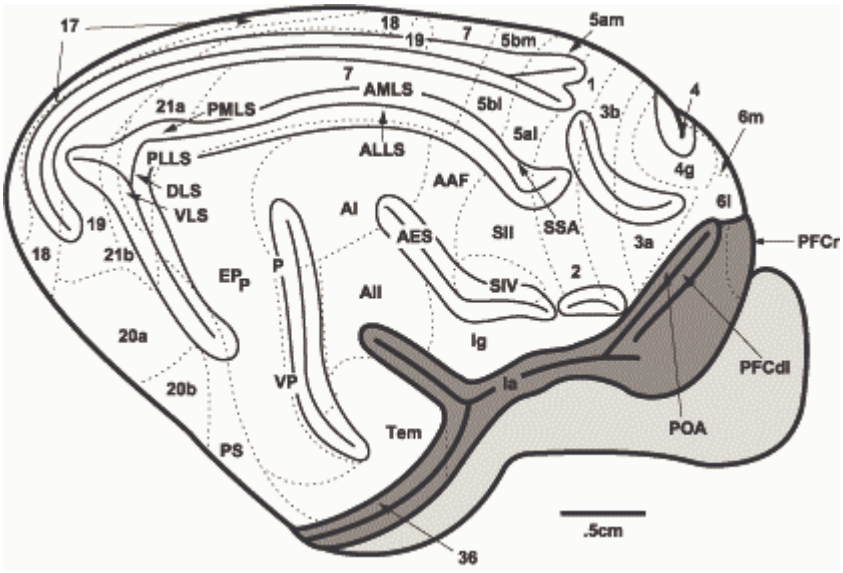

Fig. S4 . Parcellation of cerebral cortex of cat. Placement of the interconnected functional areas is evaluated for how well total connection-costs are minimized. (A) Connection-cost optimization analysis of layout of 15 contiguous areas of the visual cortex, along with 13 immediately contiguous "edge" areas. 126 connections are reported among the core areas and with their edge areas. (B) Similar combined analysis of 39 areas of the visual, auditory, and somatosensory cortex, along with 14 edge-areas (451 connections reported). Core and edge areas are listed in Table S2 connection matrix below. Lateral aspect only is shown. Rostral is to right.(4)

Table S2. Combined connection and adjacency matrix for cat visual, auditory, and somatosensory cortex. The series of 39 core areas as in Fig. S4 is listed, in the order in which the areas are successively added to the analysis (17 - 6l). They are followed by the set of 14 edge areas for the total core (POA - Ig). A cell with 0 indicates no known connection between the area of that row and of that column; 1 - 6 indicates connection between the two areas. (Afferent and efferent connection weights of 1 - 3 have been summed.) Cell values in **bold** designate topological contiguity of the two areas on the cortex sheet, as in Fig. S4.(5)

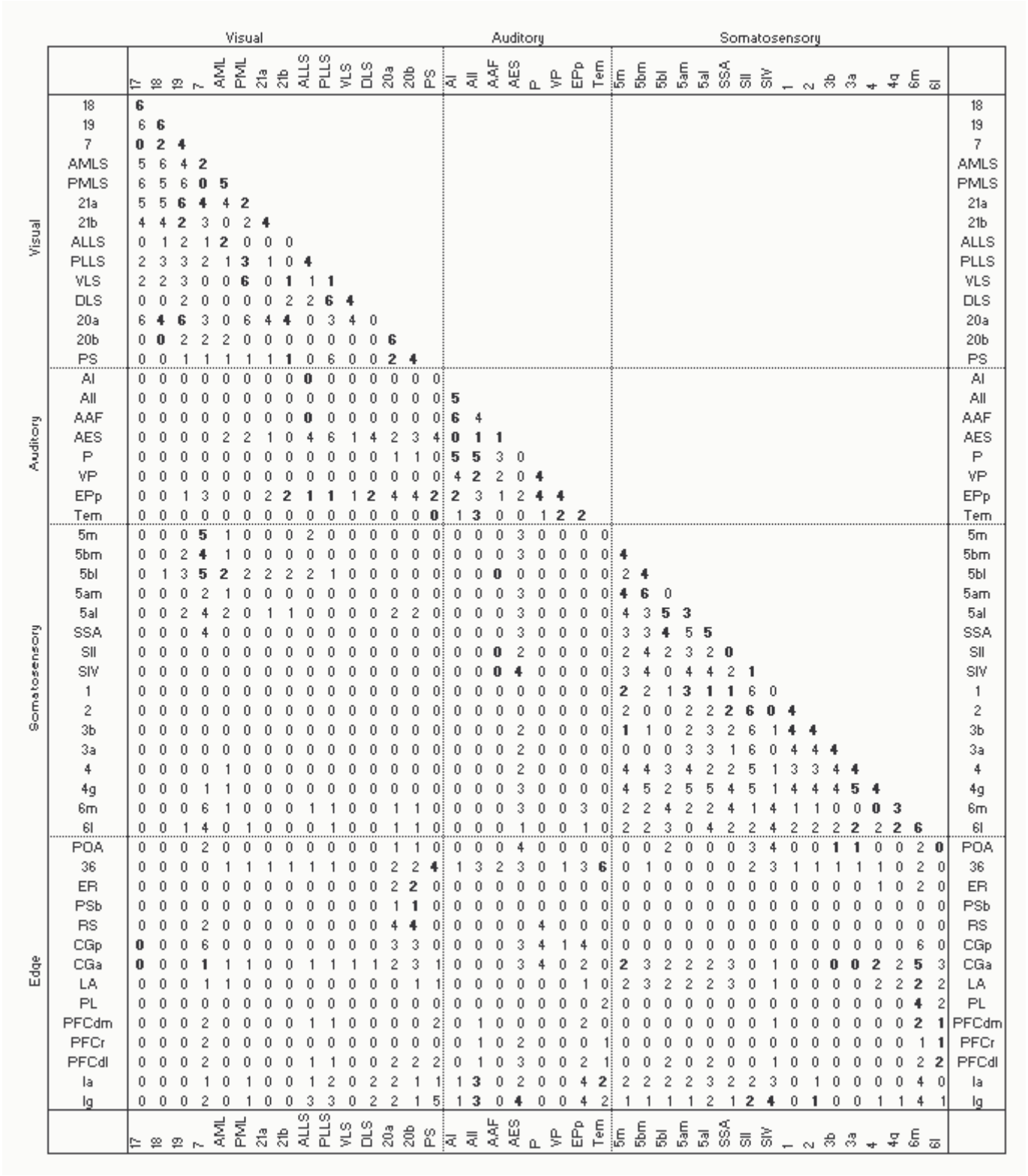
Visual
Auditory
Somatosensory
Visual
Auditory
Somatosensory
Edge
17 18 19 7 AML PML 21a 21b ALLS PLLS VLS DLS 20a 20b PS
AI AII AAF AES P VP EPp Tem
5m 5bm 5bl 5am 5al SSA SII SIV 1 2 3b 3a 4 4g 6m 6l
18 19 7 AMLS PMLS 21a 21b ALLS PLLS VLS DLS 20a 20b PS
AI AII AAF AES P VP EPp Tem
5m 5bm 5bl 5am 5al SSA SII SIV 1 2 3b 3a 4 4g 6m 6l
POA 36 ER PSb RS CGp CGa LA PL PFCdm PFCr PFCdl Ia Ig

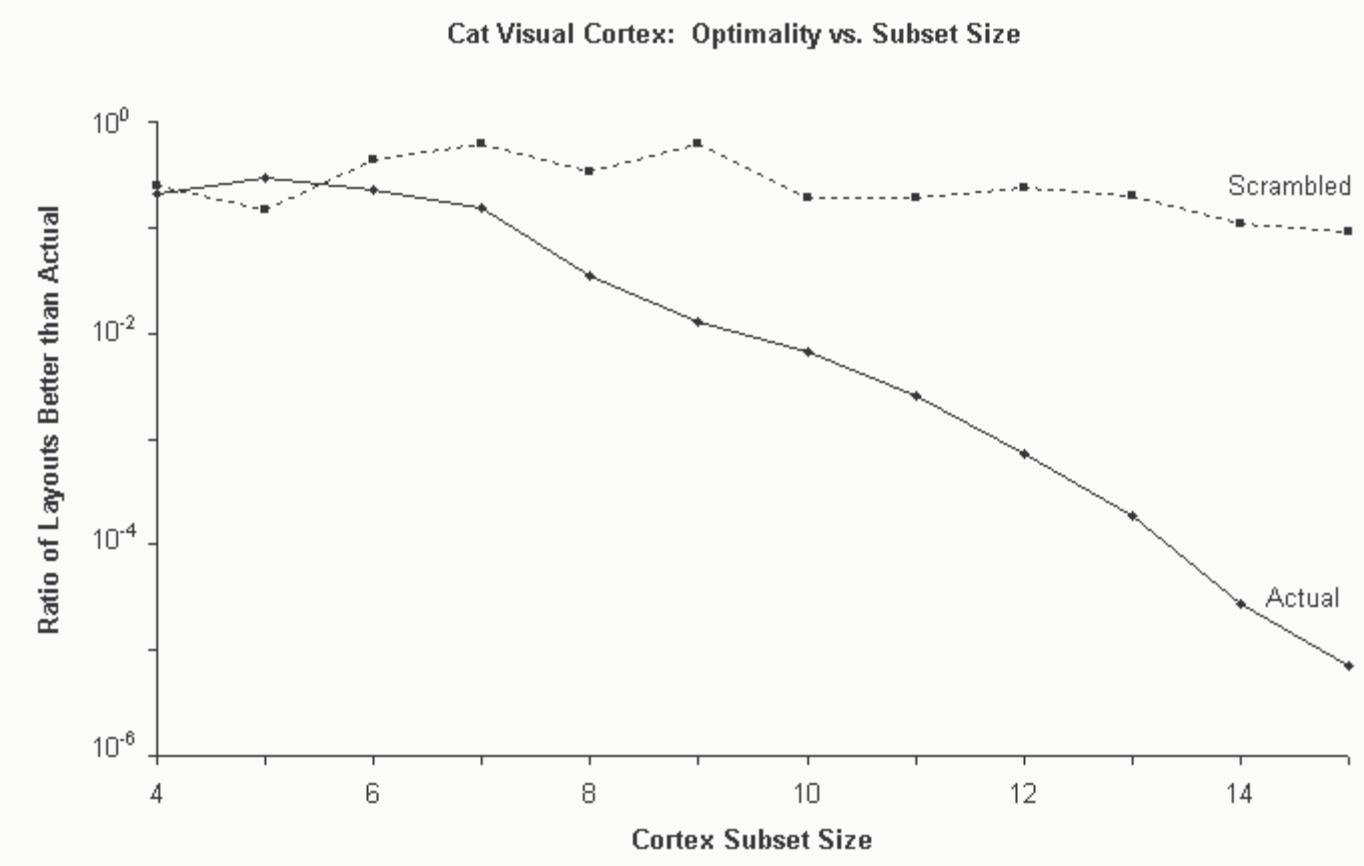

Fig. S5. Size Law for cat visual cortex areas. The system of components here is the 15 contiguous cat visual cortical areas in Fig. S4 (17 - PS), with connections and adjacencies as in Table S2. Optimality-measure is conformance of the system to the "all or nothing" adjacency rule, with each layout scored in terms of its number of violations of the rule. A series of nested compact subsets of the set of cortex areas was generated, each consisting of from 4 to the full 15 areas. Each subset of the actual layout was compared with all possible alternative layouts of that subset for adjacency-rule optimality.

The "Actual layout" curve shows that smaller subsets rank approximately in the middle of their group of alternative layouts. But, again, as subset size increases, optimality-ranking of the actual layout consistently improves (with one exception, $p < 0.02$). Only one in a hundred thousand of all alternative layouts conform to the adjacency rule better than the actual layout of the complete 15-component set. For comparison, the "Scrambled layout" broken-line curve shows the corresponding analysis for a layout of the 15 visual areas with their adjacencies randomly shuffled; no Size Law trend toward improving optimality is evident. Note that this analysis includes only 15 of the total 57 cortical areas.

Previous | Next

Table S3 . Combined connection and adjacency matrix for "metamodules" composed from areas of cat visual, auditory, and somatosensory cortex. The series of 14 metamodules, each constructed from the areas in Fig. S4 above, with connections and adjacencies from Table S2, is listed in the order in which the areas are successively added to the analysis. They are followed by the set of 13 edge areas for the total core. A cell with 0 indicates no known connection between the metamodule of that row and of that column; 1 - 44 indicates connection between the two metamodules. (Afferent and efferent connection weights of all areas in the two metamodules have been summed. A total 134 connections are included. Cell values in **bold** designate topological contiguity of the two metamodules on the cortex sheet, as in Fig. S4.

	V1	V2	V3	V4	V5	A1	A2	A3	S1	S2	S3	S4	S5	S6
V2	**12**													
V3	**9**	**23**												
V4	6	**13**	**16**											
V5	15	37	**17**	23										
A1	0	0	0	0	**0**									
A2	0	0	1	11	19	**24**								
A3	0	1	**7**	**10**	**5**	**4**	**19**							
S1	0	8	**30**	4	**14**	**0**	15	0						
S2	0	0	0	0	0	**0**	**6**	0	**30**					
S3	0	0	0	0	0	0	0	0	**18**	**12**				
S4	0	0	0	0	0	0	4	0	**16**	13	**16**			
S5	0	0	1	0	2	0	5	0	44	12	14	**17**		
S6	0	1	12	6	5	0	8	4	31	18	6	**6**	**7**	
36	0	0	2	**8**	4	3	7	**9**	1	5	2	2	1	2
ER	0	0	0	**4**	0	0	0	0	0	0	0	0	1	2
PSb	0	0	0	**2**	0	0	0	0	0	0	0	0	0	0
RS	0	0	2	**8**	0	0	4	0	0	0	0	0	0	0
CGp	**0**	0	6	6	0	0	8	4	0	0	0	0	0	10
CGa	**0**	0	**1**	6	6	0	7	2	**14**	1	0	**0**	**4**	**8**
LA	0	0	1	2	1	0	0	1	14	1	0	0	4	**4**
PL	0	0	0	0	0	0	0	2	0	0	0	0	0	**6**
PFCdm	0	0	2	2	2	0	1	2	0	1	0	0	0	**3**
PFCr	0	0	2	0	0	0	3	1	0	0	0	0	0	**2**
PFCdl	0	0	2	6	2	0	4	3	4	1	0	0	0	**4**
Ia	0	0	1	4	6	1	**5**	**6**	13	5	1	0	0	**5**
Ig	0	0	2	8	9	1	**7**	6	7	**6**	**1**	0	2	**7**

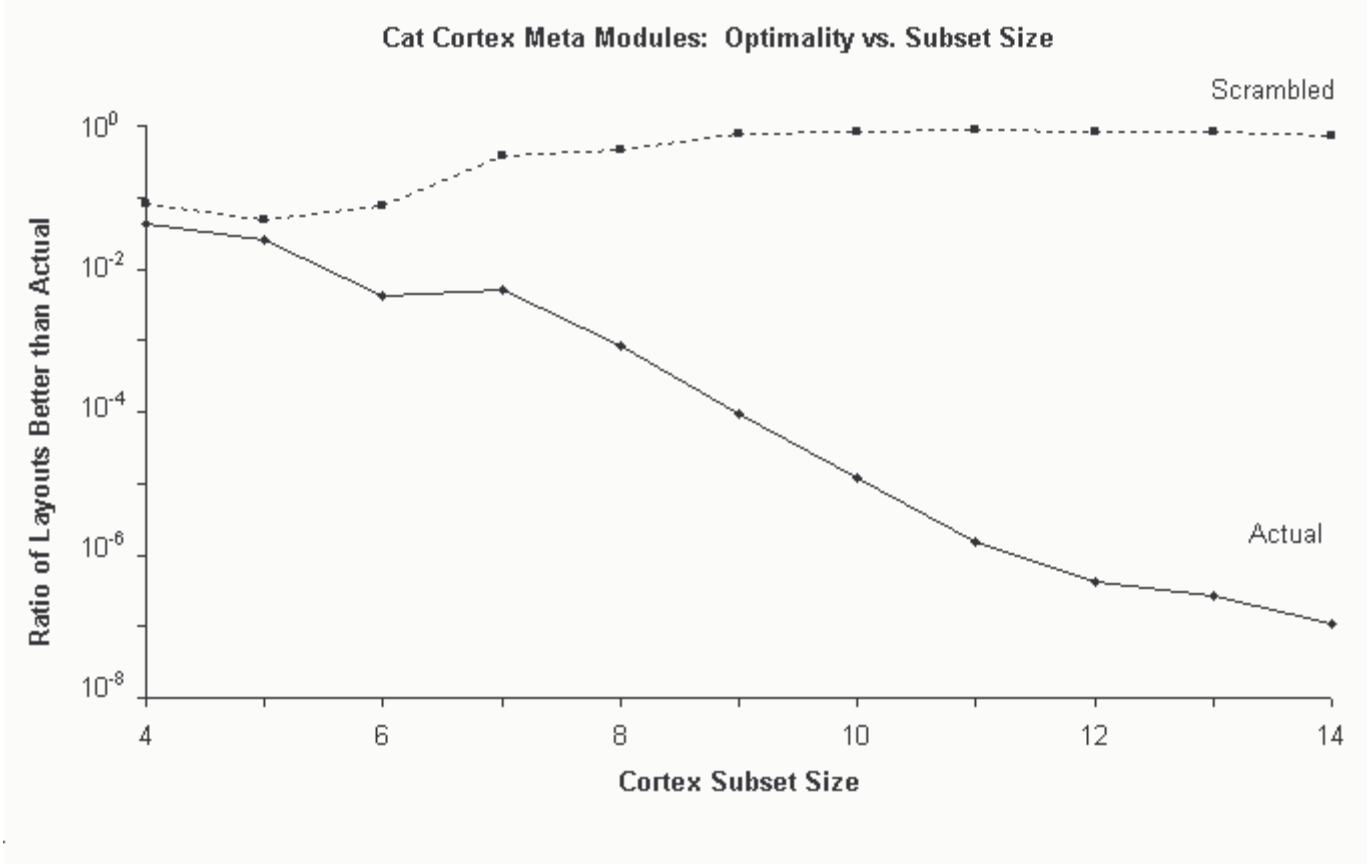

Fig. S6. Size Law for cat cortex "metamodules". If a set of connected components is optimally placed, then a set of metamodules each consisting of a subset of those components in the same positions will also be optimally placed. 40 Brodmann areas of the visual, auditory, and somatosensory regions of the cat cortex are grouped into 14 such modules, with connections and adjacencies as in Table S3. A series of nested subsets of those metamodules was then generated. The same Size Law trend of optimality improvement of the actual metamodule layout with increasing subset size is evident as for the actual layout of individual areas of the cat visual cortex: As subset size increases, optimality-ranking of actual layout consistently improves (with one exception, $p < 0.02$). (Exhaustive searches of all alternative layouts were performed.)

However, since 40 individual areas are now incorporated in these 14 metamodules, the Size Law furthermore implies that such a larger subset of the total 57-area cortical system should show better optimization than the 15-area visual subset. Such improvement is evident here: For example, by a subset size of 11 metamodules (consisting of 31 cortical areas), the actual layout's top ~10^{-6} rank exceeds the full 15-area visual system's rank; the full 14-metamodule actual layout ranks in the top 1.09×10^{-7} of all 14! possible alternative layouts--almost 100 times better than the full 15-area visual system. "Scrambled layout" broken-line curve shows corresponding analysis for a randomly shuffled layout of the meta-modules; no Size Law trend is evident.

Previous | Next

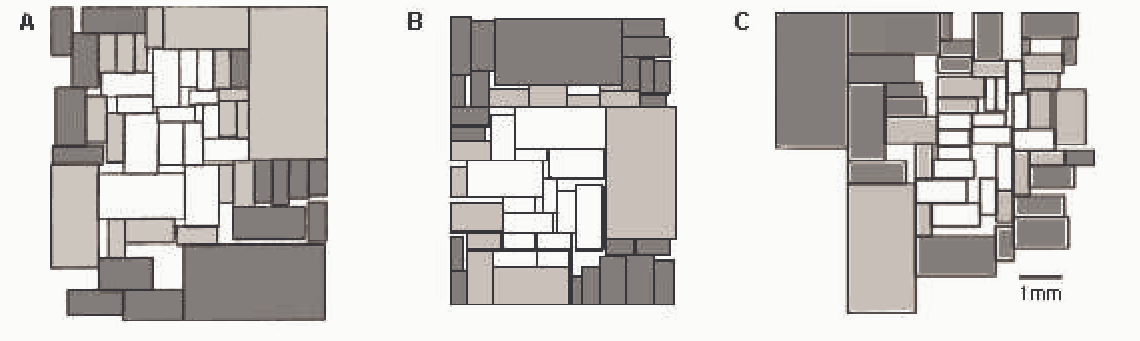

Fig. S7 . Integrated circuit networks for calibration of optimality analysis: AMI49 microchip, the largest of the MCNC set of benchmark circuits, with 49 modules.(6) (**A**) Esbensen and Kuh layout; cost to be minimized is a function of layout area and maximum path delay.(7) (**B**) Hong et al layout; cost to be minimized is a function of area and total wirelength.(8) (**C**) Lin and Chang layout; cost to be minimized is total wirelength.(9) In each case, the central 15 blocks (white), along with the surrounding edge-zone of immediately contiguous blocks (light gray), was analyzed. Again, placement of the interconnected areas is evaluated for how well total interconnection costs--adjacency rule violations--are minimized. Core and edge areas for Lin and Chang layout are listed in Table S4 connection matrix below.

Table S4. Combined connection and adjacency matrix for Lin and Chang layout of AMI49 microchip. The series of 15 core blocks shown above in Fig. S7C is listed (M014 - M020), in the order in which the areas are successively added to the analysis. They are followed by the set of 14 edge blocks for the total core (M030 - M032). (There are 103 connections among the core blocks and with the edge blocks.) A cell with 0 indicates no connection between the area of that row and of that column; 1 - 14 indicates connection density between the two areas. Cell values in **bold** designate topological contiguity of the two areas on the chip, as in Fig. S7C.

	1	2	3	4	5	6	7	8	9	10	11	12	13	14	15
	M014	M025	M021	M017	M016	M036	M037	M034	M035	M031	M029	M041	M039	M024	M020
M025	**4**														
M021	**1**	**4**													
M017	0	0	**0**												
M016	0	2	0	**10**											
M036	4	5	1	0	**0**										
M037	0	0	0	0	0	**0**									
M034	0	2	0	0	0	6	**0**								
M035	0	0	0	0	0	2	0	**8**							
M031	0	1	1	0	0	3	0	3	**2**						
M029	0	2	1	0	0	1	0	0	0	**1**					
M041	0	0	0	0	0	0	0	0	0	0	**0**				
M039	0	0	0	0	0	0	13	0	0	0	0	**0**			
M024	0	1	1	0	0	2	0	0	0	1	1	0	**0**		
M020	0	0	2	0	0	0	0	0	0	0	0	0	0	**0**	
M030	2	0	0	0	2	2	0	4	2	14	**0**	0	0	2	0
M004	0	1	1	0	0	0	**0**	1	0	0	0	0	0	0	0
M049	0	0	0	0	0	1	0	0	**0**	**0**	0	0	0	0	0
M018	1	2	2	9	0	1	0	0	0	**1**	**1**	0	0	1	0
M027	0	3	0	0	0	2	0	1	0	0	**4**	2	0	0	0
M046	0	1	0	0	0	0	0	0	0	0	0	1	0	0	0
M043	0	0	0	0	0	0	0	1	0	0	0	**7**	0	0	0
M040	0	2	1	0	0	1	0	0	0	1	2	0	**0**	1	0
M038	0	2	1	0	0	1	5	0	0	1	1	0	**12**	1	0
M019	1	5	6	1	0	2	1	1	0	1	1	0	**0**	**3**	**2**
M023	0	0	4	0	0	0	0	0	0	0	0	0	0	6	**0**
M022	0	**2**	**1**	0	0	0	0	0	0	0	0	0	0	0	0
M008	0	1	**1**	**0**	0	2	0	0	0	1	1	0	0	1	0
M015	1	1	1	0	2	**1**	**0**	0	0	0	0	1	0	0	0
M032	4	4	2	0	0	9	**0**	**5**	0	1	1	0	0	2	0

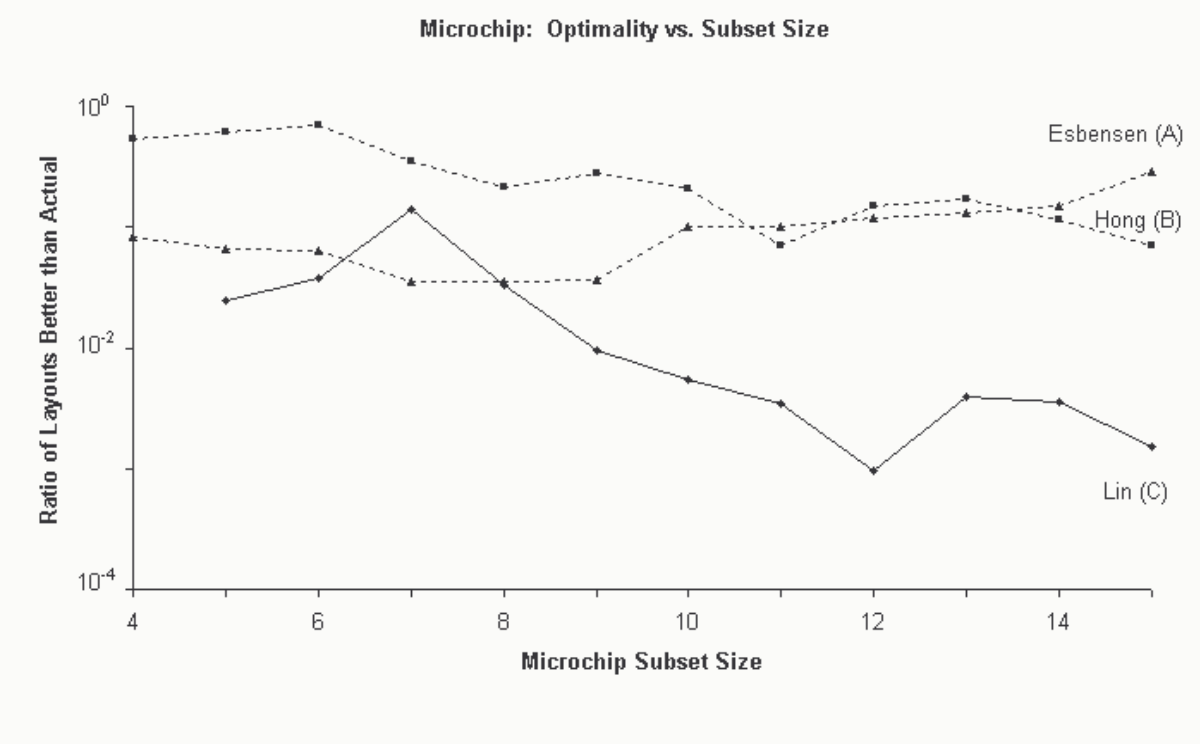

Fig. S8. Size Law for three layouts of AMI49 chip. In each case, the system of components is 15 contiguous central blocks as in Fig. S7; connections and adjacencies for Lin and Chang are as in Table S4. Optimality-measure is conformance of the system to the adjacency rule, with a layout scored in terms of number of violations of the "all or nothing" adjacency rule. A series of nested compact subsets of the set of blocks was generated, each consisting of from 4 to the full 15 areas. (For the Lin and Chang layout, order of successive elements added is as in Table S4.) Each subset of the actual layout was compared with all possible alternative layouts of that subset for adjacency-rule optimality (14 and 15-element sets were each compared only with random samples of 10^9 alternative layouts).

The curve for the Lin and Chang layout (**C**) shows the same Size Law pattern as the cortex networks earlier, although somewhat weaker; the full 15-component subset only attains an optimality-rank of 1.5×10^{-3}. Both Esbensen and Kuh (**A**), and Hong et al (**B**), layouts do not show a Size Law pattern, nor does either attain significant optimality. So, for these calibration networks, adjacency rule conformance seems capable of distinguishing wirelength minimization from some other related cost-measures. Note that the analysis includes only 15 of the total system of 49 modules. (See also Fig. S1 above.)

Previous | Next

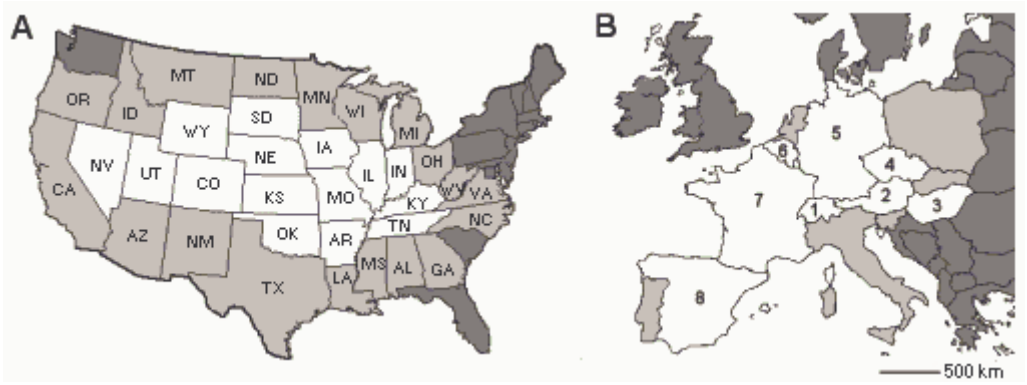

Fig. S9. Macroeconomic commodity-flow networks. (A) U.S. interstate commodity flow.(10) The central 15 states (white), along with the surrounding edge-zone of 19 immediately contiguous states (light gray), were analyzed. Core and edge areas for USA15 states are listed in Table S5 connection matrix below. (B) European international commodity flow.(11) The central 8 countries (white), along with a fragmentary surrounding edge-zone of 6 immediately contiguous countries (light gray), were analyzed as pilot data.

Table S5. Combined "connection" and adjacency matrix for U.S. interstate commodity flow (1997 Survey Sample). The series of 15 core states shown above in Fig. S9A is listed (KS - OK), in the order in which the areas are successively added to the analysis. They are followed by the set of 19 edge states for the total core (TX - LA). Cell values are in $ millions. An all-or-nothing cutoff threshold was set to yield approximately the same connectivity density as macaque and cat cortex above (see Table S7): If "export" + "import" flow between two states exceeds $ 1,500,000,000, a connection is recorded; sub-threshold economic transactions between the state of a row and the state of a column count as no connection. Cell values in bold designate topological contiguity of the two states, as in Fig. S9A.

	KS	CO	UT	NV	WY	SD	NE	IA	MO	IL	IN	KY	TN	AR	OK
CO	**2885**														
UT	755	**2976**													
NV	26	824	**3507**												
WY	258	**2113**	**826**	137											
SD	344	653	401	0	**146**										
NE	**4384**	**2623**	410	0	**449**	**1373**									
IA	3242	1582	536	255	224	**2029**	**7700**								
MO	**15773**	2987	1605	360	453	144	**3225**	**6793**							
IL	5971	4794	1010	893	551	842	4964	**17277**	**24981**						
IN	2234	1715	892	429	269	598	1659	4900	10785	**36898**					
KY	1175	1152	798	319	6	58	457	1656	**3700**	**9578**	**13761**				
TN	2011	1585	799	548	71	250	775	2377	**5735**	10844	8345	**12690**			
AR	1590	628	362	250	181	36	570	1511	**7237**	4562	2993	2191	**6246**		
OK	**3896**	**1382**	516	237	364	51	815	1598	**3850**	3231	1343	869	1854	**3685**	
TX	9197	8826	3136	1608	556	933	4920	6021	13838	26051	14220	9133	13514	**12630**	**20480**
NM	219	**1512**	464	193	45	0	240	141	465	610	440	313	246	183	**402**
AZ	1198	2029	**2075**	**2457**	84	0	418	874	2317	2321	1730	700	2079	1053	577
CA	8542	15459	10888	**20494**	470	1797	5191	6160	15928	29183	10677	11997	12958	6649	7849
OR	633	1748	1192	**824**	438	199	495	926	1197	3138	2485	1188	1099	513	559
ID	345	1191	**2732**	**676**	**258**	48	310	303	363	949	316	60	322	103	32
MT	235	804	678	152	**630**	**343**	248	477	91	772	304	123	198	166	351
ND	2635	2778	1885	682	223	**191**	2887	4828	13442	30441	30737	12361	9542	2062	3004
MN	256	67	32	3	47	**848**	325	**1134**	403	1308	524	0	304	179	205
WI	2104	1834	1005	304	259	3862	3160	**9345**	3957	**16164**	4928	2293	3003	1319	1446
MI	2485	2905	1098	733	303	1570	1901	6815	4898	32094	**7644**	3271	5070	1628	1795
OH	4279	3082	2076	1148	192	668	2334	6774	9986	32937	**33056**	**20618**	7652	3691	1754
WV	163	34	70	18	19	7	78	133	699	1732	1161	**2950**	1277	158	88
VA	779	1758	608	256	63	163	809	1485	2289	6499	3385	**5273**	**7368**	1164	1597
NC	2216	1578	375	545	86	126	1020	2392	5148	9085	5549	5883	**10623**	2096	1622
GA	1929	1883	1189	568	139	97	1242	2506	7432	11852	7164	6451	**19411**	3620	1558
AL	965	393	218	18	39	66	269	934	2528	4853	3976	3138	**10948**	2096	995
MS	652	380	261	88	5	204	579	706	1941	3209	2035	1668	**7364**	**4227**	816
LA	1161	576	167	145	154	4	436	2660	3046	9494	3352	3628	4813	**4880**	1876

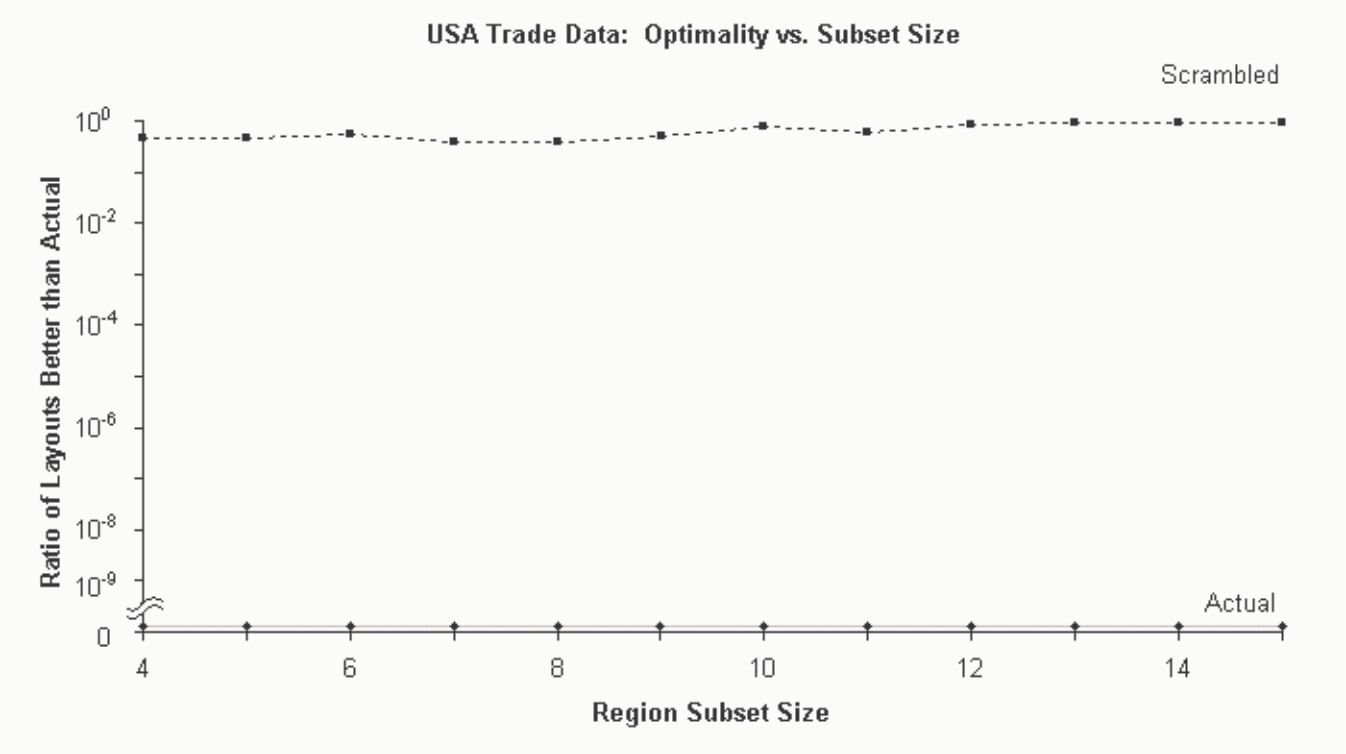

Fig. S10. Size Law performance for commodity flow among 15 U.S. states (BTS). The system of components here is a core of contiguous economic zones as in Fig. S9, with "connections" and adjacencies as in Table S5. For evaluation of how well total interconnection costs are minimized, optimality-measure is conformance of the system to the "all or nothing" adjacency rule: each layout is scored in terms of its number of violations of the rule. A series of nested compact subsets of the set of zones was generated (order of successive states added is as in Table S5). Each subset of the actual layout was compared with all possible alternative layouts of that subset for adjacency-rule optimality (14 and 15-element sets were each compared only with random samples of 10^9 alternative layouts).

The US system attains better connection-optimization than macaque or cat visual cortex, with no layouts better than actual found in a 1 billion sample. This may appear to vindicate the "invisible hand" of laissez-faire economics. However, the "Actual layout" curve departs markedly from the Size Law pattern; smaller subsets already attain perfect optimality--i.e., an optimality ratio of 0, with no alternative layouts better than the actual one. This breakdown suggests the macroeconomic networks are optimized locally, unlike the cortex (and some chip) networks. For calibration, the "Scrambled layout" (broken-line) curve, for the 15 U.S. states with their adjacencies randomly shuffled, shows the usual "flat" unoptimized pattern.

Previous | Next

Table S6. Component placement optimization: results summary. "Estimated Rank" designates proportion of all possible alternative layouts that are of lower connection-cost than the actual layout. Each layout is scored for violations of the Adjacency Rule. Size Law goodness of fit r^2 is for a model of the form of an inverse exponential function $y = ke^{-mx}$.

	Number of Components	Estimated Rank	Size Law r^2
Neural Networks			
Caenorhabditis elegans	11	$4.0\ 10^{-7}$	0.99
Macaque Visual Cortex	17	$1.2\ 10^{-7}$	0.91
Cat Visual Cortex	15	$7.2\ 10^{-6}$	0.94
Cat Cortex Metamodules	14	$1.1\ 10^{-7}$	0.97
Cat Cortex:			
Vis, Aud, Somato	39	$[(3x)\ 10^{11}]$*	---
Non-Neural Networks			
AMI49 Microchip			
Esbenson & Kuh Layout	15	$7.0\ 10^{-2}$	0.77
Hong et al Layout	15	$3.3\ 10^{-1}$	0.69
Lin & Chang Layout	15	$1.5\ 10^{-3}$	0.78
Macroeconomic Networks			
USA Commodity-Flow	15	---	---
Europe Ex/Im	8	$4.0\ 10^{-4}$	---

*In each of 3 separate replications, 100 billion randomly sampled layouts were tested without finding a better layout than the actual one.

Table S7. Connections vs adjacencies among network components: 2 x 2 contingency tables. For each neural system, the relationship is highly significant: $p < 0.0001$; $r > 0.30$. Connections and adjacencies to immediately contiguous edge-components are included. (Number of core components is given in parentheses.)

Cortex Networks

Macaque Visual Cortex (17)

	Adj	NotAdj	Total	X^2	*r*
Con	38	82	120	30.6433	0.30801
NotCon	16	187	203		
Total	54	269	323		

Cat Visual Cortex (15)

	Adj	NotAdj	Total	X^2	*r*
Con	40	86	126	40.0761	0.365496
NotCon	8	166	174		
Total	48	252	300		

Cat Metamodules (14)

	Adj	NotAdj	Total	X^2	*r*
Con	44	90	134	37.09234	0.368605
NotCon	6	133	139		
Total	50	223	273		

Cat Vis/Aud/Som Cortex (39)

	Adj	NotAdj	Total	X^2	*r*
Con	101	350	451	143.0408	0.333381
NotCon	18	818	836		
Total	119	1168	1287		

Non-Neural Networks

AMI49 Microchip

Esbensen & Kuh Layout (15)

	Adj	NotAdj	Total	X^2	*r*
Con	17	95	112	0.62703	0.0409
NotCon	32	231	263		
Total	49	326	375		

Hong et al Layout (15)

	Adj	NotAdj	Total	X^2	*r*
Con	14	86	100	0.00072	0.0016
NoCon	24	146	170		

Total	38	232	270

Lin & Chang Layout (15)

	Adj	NotAdj	Total	X^2	*r*
Con	19	84	103	6.62842	0.1451
NotCon	18	194	212		
Total	37	278	315		

Macroeconomic Networks

USA Commodity-Flow (15) (@1500)

	Adj	NotAdj	Total	X^2	*r*
Con	47	137	184	29.4310924	0.274708
NotCon	12	194	206		
Total	59	331	390		

Europe Ex/Im (8) (@1250)

	Adj	NotAdj	Total	X^2	*r*
Con	23	36	59	8.06358	0.3098
NotCon	2	23	25		
Total	25	59	84		

Previous | Next

References and Notes

1. Worm nervous system wiring data is as reported in: Cherniak, C. (1994) Component placement optimization in the brain. Journal of Neuroscience 14: 2418-2427 (1994). (See also: Network Optimization in the Brain: Cerebral Cortex Layout [II: 2/2000] NIMH Grant Application, UMIACS Tech Report CS-TR-4525 . www.cs.umd.edu/Library/TRs/)

2. Diagram adapted with revisions from: Felleman, D., and Van Essen, D. (1991) Distributed hierarchical processing in the primate cerebral cortex. Cerebral Cortex 1: 1-47. (Fig. 2, p. 4); Van Essen, D., et al (1990) Modular and hierarchical organization of extrastriate visual cortex in the macaque monkey. Cold Spring Harbor Symposia on Quantitative Biology LV: 679-696 (Fig. 6, p. 689). Areas MIP and MDP are included in PO.

3. Connections based upon: Scannell, J. (1997) Determining cortical landscapes. Nature 386: 452. www.psychology.ncl.ac.uk/jack/gyri.html; from Young, M. (1993) The organization of neural systems in the primate cerebral cortex. Proceedings of the Royal Society, B 252: 13-18. Adjacencies from Felleman and Van Essen (1991) (see note 2). Adjacencies do not include "diagonals", where only corners of two areas are contiguous (e.g., V3a and LIP in Fig. 2); similarly for all analyses below. (Because of incomplete information, the edgering has a gap at PS, 29, 30.)

4. Diagram based upon: Scannell, J., Blakemore, C., and Young, M. (1995) Analysis of connectivity in the cat cerebral cortex. Journal of Neuroscience 15: 1463-1483. (Fig. 1, p. 1466; with corrections.) Area SVA is included in 17, ALG in 19; DP in EPp & AI, V in VP & AII, SSF in EPp; a number of boundary indeterminacies remain unresolved.

5. Connections and adjacencies based upon Scannell et al (1995) (see note 4). Adjacencies do not include "diagonals", where only corners of two areas are contiguous.

6. Connection matrix of AMI49: Benchmark suite LayoutSynth92 1992 International Workshop on Layout Synthesis, North Carolina. www.cbl.ncsu.edu/pub/Benchmark_dirs/LayoutSynth92/bench90.tar.Z

7. Diagram based upon: Esbensen, H., and Kuh, E. A performance-driven IC/MCM placement algorithm featuring explicit design space exploration. ACM Trans. Design Automation of Electronic Systems, vol. 2, no. 1 (January 1997), p. 79, Figure 9(b). info.acm.org/todaes/V2N1/L134/paper.pdf

8. Diagram based upon: Hong, X., Huang, G., Cai, Y., Dong, S., Cheng, C., and Gu, J. Corner block list: An effective and efficient topological representation of non-slicing floorplan. Int. Conf. Computer-Aided Design, Nov.2000, pp. 8-12. www.cse.ucsc.edu/research/surf/GSRC/Papers/01a_2.pdf

9. Diagram based upon: Lin, J.-M. and Chang, Y.-W. TCG: A transitive closure graph based representation for non-slicing floorplans. In Proc. of ACM/IEEE Design Automation Conference

(DAC-2001), Las Vegas, NV, June 2001. Figure 6 (2).
http://cc.ee.ntu.edu.tw/~ywchang/Papers/tcg01.ps

10. State-to-State Commodity Flows: Commodity Flow Survey (1997). Bureau of Transportation Statistics, U.S. Department of Transportation. www.bts.gov/ntda/cfs/docs/cf97odv.html

11. International Trade by Commodity Statistics (1999). Organisation for Economic Co-operation and Development. www.oecd.org/xls/M00017000/M00017616.xls
(See also: Richardson, L. Statistics of Deadly Quarrels (Boxwood Press, Pittsburgh, 1960)) ch. 5.4.)

This work was supported by NIMH grant MH49867. NCI generously made available supercomputers at their Advanced Biomedical Computing Center. We thank Richard Kissh for parallel supercomputer software engineering. We are also grateful for assistance of Eric Celarier, Jarrett Rosenberg, Thomas Schaefer, and Corey Washington.

Previous | Home